

See discussions, stats, and author profiles for this publication at: <https://www.researchgate.net/publication/234082817>

Specific Cation Effects on the Bimodal Acid–Base Behavior of the Silica/Water Interface

ARTICLE *in* JOURNAL OF PHYSICAL CHEMISTRY LETTERS · APRIL 2012

Impact Factor: 7.46 · DOI: 10.1021/jz300255x

CITATIONS

19

READS

57

3 AUTHORS, INCLUDING:



Md Shafiul Azam

Bangladesh University of Engineering and Tec...

13 PUBLICATIONS 115 CITATIONS

SEE PROFILE



Julianne M Gibbs-Davis

University of Alberta

37 PUBLICATIONS 748 CITATIONS

SEE PROFILE

Specific Cation Effects on the Bimodal Acid–Base Behavior of the Silica/Water Interface

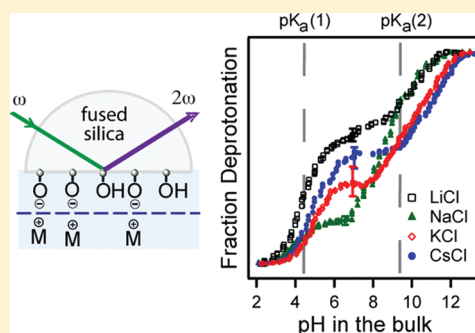
Md. Shafiul Azam, Champika N. Weeraman, and Julianne M. Gibbs-Davis*

Department of Chemistry, University of Alberta, Edmonton, Alberta, Canada

Supporting Information

ABSTRACT: Using nonresonant second harmonic generation spectroscopy, we have monitored the change in surface charge density of the silica/water interface over a broad pH range in the presence of different alkali chlorides. Planar silica is known to possess two types of surface sites with pK_a values of ~ 4 and ~ 9 , which are attributed to different solvation environments of the silanols. We report that varying the alkali chloride electrolyte significantly changes the effective acid dissociation constant (pK_a^{eff}) for the less acidic silanol groups, with the silica/ NaCl_{aq} and silica/ CsCl_{aq} interfaces exhibiting the lowest and highest pK_a^{eff} values of 8.3(1) and 10.8(1), respectively. Additionally, the relative populations of the two silanol groups are also very sensitive to the electrolyte identity. The greatest percentage of acidic silanol groups was 60(2)% for the silica/ LiCl_{aq} interface in contrast to the lowest value of 20(2)% for the silica/ NaCl_{aq} interface. We attribute these changes in the bimodal behavior to the influence of alkali ions on the interfacial water structure and its corresponding effect on surface acidity.

SECTION: Surfaces, Interfaces, Porous Materials, and Catalysis



Understanding the interactions of cations with mineral oxides is of central importance in predicting geochemical processes such as deprotonation,¹ dissolution,² and adsorption.³ Indeed, the accuracy of pollutant transport models depends on correctly identifying the influence of common spectator ions such as sodium and potassium on geochemical systems involving mineral oxides.^{4–8} In addition to the environmental significance, the behavior of insulating mineral oxides such as silica is also pertinent to applications ranging from catalysis⁹ to diagnostics^{10,11} as such oxides are often used as the support material. In particular, the binding affinity of the mineral oxide interface for aqueous species is often influenced by the surface charge density as a result of electrostatic interactions.⁴ Consequently, there has been a great deal of work aimed at quantifying the acid–base equilibria of silica, and a range of pK_a values has been reported that vary depending on silica morphology.^{1,8,12–15} However, despite the large amount of attention, the influence of specific ions on the acid–base behavior of planar silica over a broad pH range has not been quantified, although planar silica exhibits two distinct equilibria between pH 2 and pH 13.

Over the past decade, interest in specific ion effects has often focused on the influence of ion polarizability on the interfacial structure of water at air/aqueous electrolyte and Langmuir–Blodgett interfaces.^{7,16–22} More recent work has turned to identifying the water structure of the solid/liquid interface and the role of specific ions at mineral oxide surfaces.²³ For example, at the fused silica/water interface, the extent of hydrogen-bonding and ordering of interfacial water was found to depend on the polarizability of the alkali ion,²³ which had

been observed at the air/water interface.¹⁸ The properties of silica are also influenced by the presence of different specific ions. The nature of the alkali ion was found to influence the surface charge density^{1,20} and zeta potential^{24,25} of colloidal silica, indicating that the charge of mineral oxides cannot be predicted from pH alone. In the former example, Ninham and co-workers were able to predict the changes in surface charge density over a narrow pH range in the presence of $\text{LiCl}_{\text{(aq)}}$, $\text{NaCl}_{\text{(aq)}}$, or $\text{KCl}_{\text{(aq)}}$ by incorporating ion polarizability, hydration, and alkali–chloride ion-pair interactions into their silica surface model.²⁰ Nevertheless, a complete picture has yet to emerge regarding the effect of the electrolyte identity on the bimodal acid–base equilibria of the planar silica/water interface. Determining specific ion effects on the surface charge density and the corresponding acid–base equilibria over a broad pH is critical to understand and predict the behavior of silica under environmentally relevant conditions.⁴ Moreover, the impact of specific cations on acid–base chemistry could prove general for other biological or material interfaces, where water–ion, water–surface, and ion–surface interactions are thought to play major roles.³³

Monitoring the acid–base behavior of insulating mineral oxides often relies on indirect measurements using pH-sensitive molecules with spectroscopic signatures^{26–28} or potentiometric titration techniques that only operate over a limited pH range.¹ However, in 1992, Eiseenthal and co-workers demonstrated that

Received: March 3, 2012

Accepted: April 24, 2012

Published: April 24, 2012

nonresonant second harmonic generation (SHG) spectroscopy provided a surface-sensitive and label-free method of monitoring the acid–base behavior of silica.²⁹ Herein we apply SHG to identify the role of specific ions on the acid–base equilibria at the silica/water interface. Our results indicate that the nature of the alkali ion has a dramatic effect on the equilibrium behavior and silanol speciation at the silica/water interface.

Within the electric dipole approximation, SHG is expected to only arise in environments where inversion symmetry is broken.¹³ For fused silica and bulk water, SHG occurs when light of frequency ω interacts with the interface of the two media causing an induced polarization that oscillates at twice the incident frequency ($P_{2\omega}$). As a result of this induced polarization, a new electric field is generated at 2ω , which emanates coherently from the interface ($E_{2\omega}$). The intensity of this response is a function of the incident electric field (E_ω) and the second-order susceptibility, $\chi^{(2)}$, which is nonzero at the interface and depends on the composition, orientation, and order of interfacial molecules.¹³ Additionally, $E_{2\omega}$ is also modulated by the presence of a third static electric field arising from charged sites at the surface according to the third-order susceptibility, $\chi^{(3)}$.^{29,30} Consequently, $E_{2\omega}$ can be expressed as

$$E_{2\omega} \propto P_{2\omega} = \chi^{(2)} E_\omega E_\omega + \chi^{(3)} E_\omega E_\omega \Phi \quad (1)$$

where Φ_0 is the interfacial potential that depends on this static electric field.¹³ At high salt concentrations, the change in interfacial potential varies linearly with surface charge density according to the constant capacitance model.⁶ At the silica/water interface, the interfacial potential is generally pH sensitive, as deprotonation of the surface above the point of zero charge (pzc ~ 2) occurs over a wide pH range. In contrast, $\chi^{(2)}$ and $\chi^{(3)}$ are considered to be much less sensitive to changes in pH.^{13,31} Consequently, the change in $E_{2\omega}$ can be directly correlated with deprotonation of the interface.^{8,13}

Figure 1 illustrates the origin of the expected increase in the SHG intensity as silica surface sites are deprotonated owing to the increase in magnitude of the interfacial potential, even in the presence of screening electrolyte.²⁹ This planar silica/water interface has been shown by SHG and other methods to exhibit two distinct acidic sites.^{26,28–30,32,33} One explanation for the two acidic sites attributes the more acidic site to silanols in contact with weakly hydrogen-bonded water (Figure 1B) and the less acidic site to silanols in contact with strongly hydrogen-bonded water (Figure 1C), which is supported by sum frequency generation experiments.^{33,34} Other researchers have suggested that the more acidic site is silanolium (protonated silanol)³⁵ or silanols lacking hydrogen bonds.²⁶ However, recent ab initio molecular dynamics simulations lend support to the role of interfacial water, finding that silanol groups on hydrophobically restructured quartz exhibited the lowest pK_a .¹⁴ They also observed that the pK_a of silanols increased as the number of water layers increased.¹⁴ Finally, the less acidic sites exhibit a $pK_a \sim 9$, which is similar to that of the monomeric form of silica, monosilicic acid ($pK_a(\text{Si}(\text{OH})_4) = 9.9$),¹² which also supports that strong solvation decreases silanol acidity. On the basis of the apparent role of water on surface acidity, we expected that the perturbation of the water structure by the alkali ions would affect the corresponding acid–base equilibrium of the silica interface.

To determine the role of specific ions on the acid–base chemistry of planar silica, we performed multiple SHG titration

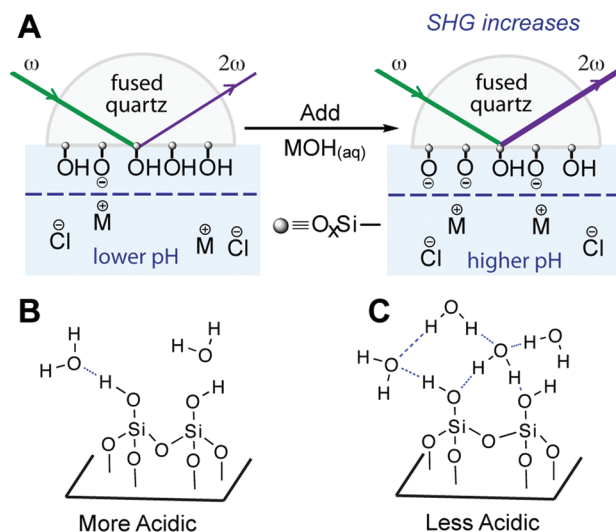
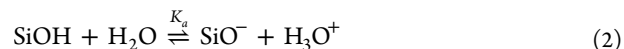


Figure 1. (A) Schematic illustrating how increasing the pH will deprotonate acidic sites causing an increase in the SHG intensity (proportional to $E_{2\omega}^2$). The 0-plane where the interfacial potential originates is depicted by the dashed line.⁸ There are two types of acidic groups at the interface, which are proposed to be (B) silanol groups associated with weakly hydrogen-bonded water resulting in a $pK_a \sim 4$ –5 and (C) silanol groups associated with strongly hydrogen-bonded water resulting in a pK_a of ~ 9 .

experiments in the presence of 0.5 M alkali chloride. Representative acid–base titration curves are shown in Figure 2 and illustrate the pH dependence of the normalized SHG electric field, which is proportional to the fraction of deprotonated silanols at the interface. As expected, the silica/water interface exhibited two distinct acidic sites: one site that dissociated below pH 7, and the other that dissociated above pH 7 (Figure 2A and B, respectively). For the more acidic silanol groups deprotonated below pH 7, we observed slight differences in behavior for all of the silica/alkali chloride electrolyte interfaces (Figure 2A). However, at higher pH, the titration profiles exhibited striking shifts in the inflection point, which revealed that the stability of these less acidic silanols depended strongly on the local electrolyte (Figure 2B). For example, in the presence of NaCl, half of these less acidic silanol groups were deprotonated at pH 8.6(1). By contrast, the corresponding point in the titration curve occurred at pH 11.1(1) in the presence of CsCl, indicating that this interface was much less acidic.

Although one cause of these specific ion effects involves altering the interfacial water structure and the corresponding surface acidity (vide supra),^{14,29,33} we can also envision that the different cations stabilize the siloxide form of surface sites to varying extents, thereby influencing silanol acidity. To quantify this effective pK_a (pK_a^{eff}), we propose a simple model based on the affinity of the alkali ion for the siloxide sites that are generated after deprotonation. We first consider the acid dissociation of the surface silanol groups leading to the corresponding siloxide conjugate base:



The cation, M^+ can then coordinate to the siloxide through electrostatic interactions.



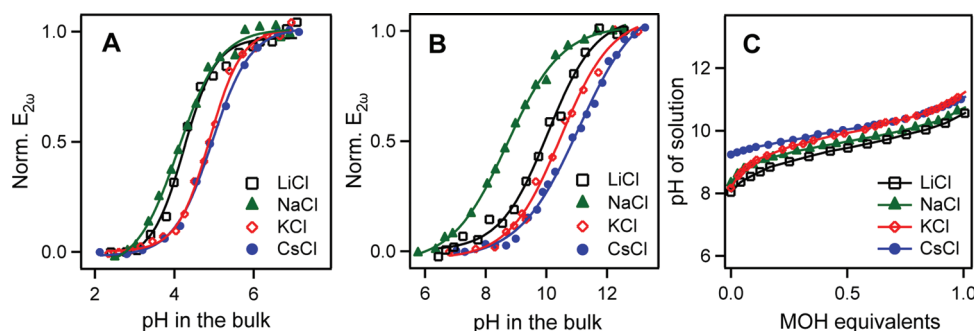


Figure 2. Representative titration curves of normalized $E_{2\omega}$ proportional to the fraction of deprotonated groups as a function of (A) low pH and (B) high pH for the silica/water interface in the presence of 0.5 M alkali chloride electrolyte. The solid lines represent the fit of a sigmoidal function to the data. (C) Representative titrations of pH versus aqueous alkali hydroxide (MOH) equivalents added to the corresponding alkali bicarbonate (initially at 0.1 M).

This electrostatic interaction does not neutralize the surface charge, which would lead to no change in the SHG signal; consequently, it must be considered a screening interaction that is specific for the siloxide sites.⁸ Finally, the overall equilibrium expression is

$$K_a^{\text{eff}} = K_a K_{\text{assc}} = \frac{[\text{SiO}^- \cdot \text{M}^+][\text{H}_3\text{O}^+]}{[\text{SiOH}][\text{M}^+]} \quad (4)$$

Owing to the relationship between $E_{2\omega}$ and the surface charge density, the pH where $E_{2\omega}$ is equal to 0.5 occurs when $[\text{SiO}^- \cdot \text{M}^+]/[\text{SiOH}]$ for a given type of silanol is one.^{29,30} The value of $\text{p}K_a^{\text{eff}}$ can then be determined from this pH ($\text{pH}_{0.5}$) and the $-\log[\text{M}^+]$, or pM^+ value, according to

$$\text{p}K_a^{\text{eff}} = \text{p}(K_a K_{\text{assc}}) = \text{pH}_{0.5} - \text{pM}^+ \quad (5)$$

It is important to note that this model does not implicitly include ion hydration or the presence of the chloride counterion, which could influence the surface behavior of the alkali ions.³ Moreover, it assumes that the surface alkali and hydronium concentrations depend similarly on their bulk concentrations such that the ratio of their surface concentrations and bulk concentrations are equal. Nevertheless, this simple model represents a good starting point for evaluating the influence of specific ions on the two acidic sites of silica based on the experimental relationship between $E_{2\omega}$ and bulk pH.

From the inflection point, $\text{pH}_{0.5}$ was determined and used to calculate $\text{p}K_a^{\text{eff}}$ values for the various alkali chlorides and the more acidic and less acidic silanol groups (Table 1, low pH and

log units, which corresponds to significant differences in silanol stability.

From hard–soft acid–base theory³⁶ we would expect that smaller hard cations should interact more strongly with the hard siloxide, leading to a higher K_a^{eff} and a lower $\text{p}K_a^{\text{eff}}$, which is indeed what we observed for both the low pH and high pH equilibria. However, for both equilibria, Na^+ rather than Li^+ exhibited the strongest affinity for the siloxide surface. In addition to the hard–soft acid–base model, another model that is useful for explaining trends in binding behavior as a function of ion polarizability is the Collins theory of matching water affinities, which suggests that ions with similar water affinities can share their hydration layer leading to ion-pair formation.³⁷ On the basis of the trend in our data, we reasoned that Na^+ and SiO^- have more closely matched water affinities than Li^+ and SiO^- , which leads to a stronger interaction between Na^+ and the surface. However, the larger shifts in $\text{pH}_{0.5}$ that we observed for the higher pH region suggested that other interactions besides those between the siloxide and cation were also critical for these less acidic silanol groups. As previously discussed, these less acidic silanol groups are thought to be stabilized in the neutral form by association with strongly hydrogen-bonded water.^{14,29,33} The presence of strongly hydrogen-bonded water and, consequently, the stability of these silanol groups should be perturbed based on the ability of the cation to disrupt the interfacial water structure.²³ Thus, we propose that the large range of $\text{pH}_{0.5}$ values for the less acidic silanols stemmed from a combination of cation stabilization of the siloxide and perturbation of the interfacial water structure. To confirm that the interfacial structure amplified these specific ion effects, we compared these results with that of a solution-phase acid in the presence of 0.5 M alkali halide. For aqueous bicarbonate, which has a $\text{p}K_a$ of 10.3,³⁸ we observed a trend in $\text{p}K_a^{\text{eff}}$ following the Hofmeister series with Li^+ rather than Na^+ leading to the lowest $\text{p}K_a^{\text{eff}}$, yet the change in $\text{p}K_a^{\text{eff}}$ was much less significant varying only by 0.6 log units (Figure 2C, Table 1). These results supported that interfaces can enhance specific ion effects, which is consistent with previous studies that concluded that specific ion effects are primarily interfacial effects.^{16,39–42}

Thus far we have considered the influence of the cation on the overall K_a^{eff} values for the more acidic and less acidic silanol groups. The relative populations of these two types of silanol groups should also be ion specific, as the presence of each type of silanol is associated with different hydrogen-bonded structures of interfacial water (Figure 1B,C).³³ Owing to the

Table 1. Salt-Dependent $\text{p}K_a^{\text{eff}}$ Values of the Silica/Water Interface and Aqueous Bicarbonate

salt	$\text{p}K_a^{\text{eff}}(\text{low-pH})$	$\text{p}K_a^{\text{eff}}(\text{high-pH})$	$\text{p}K_a^{\text{eff}}(\text{MHCO}_3)$
LiCl	4.1(2)	9.6(2)	9.13(3)
NaCl	3.76(4)	8.3(1)	9.34(4)
KCl	4.6(2)	9.9(2)	9.62(2)
CsCl	4.5(2)	10.8(1)	9.73(2)

high pH, respectively). There was not a large trend in the lower pH region for the more acidic silanol groups, but generally the K_a^{eff} values decreased with an increase in cation polarizability. The trend in K_a^{eff} values for the higher pH was more pronounced in the order $K_a^{\text{eff}}(\text{NaCl}) > K_a^{\text{eff}}(\text{LiCl}) > K_a^{\text{eff}}(\text{KCl}) > K_a^{\text{eff}}(\text{CsCl})$, with the relative position of LiCl or NaCl leading to a deviation from the Hofmeister trend. Moreover, the $\text{p}K_a^{\text{eff}}$ values for these less acidic silanols differed by more than two

ability of ions to disrupt the structure of interfacial water,²³ the relative amounts of the weakly and strongly hydrogen-bonded interfacial water should be very sensitive to the specific ion present, which in turn should influence the population distribution of the more and less acidic silanol groups. Recent SFG studies by Chou and co-workers have shown that the relative amount of strongly hydrogen-bonded, or high coordinate, water at the silica/alkali chloride electrolyte interface varied with salt concentration and cation polarizability. At electrolyte concentrations less than 0.1 M, they found that lithium was more disruptive to the strongly hydrogen-bonded water than sodium, but potassium led to the most disruption.²³ The authors attributed this lack of trend to potassium's greater affinity for the silica surface at pH 7 (from potentiometric measurements performed on colloidal silica)¹ and the hydrated lithium's greater ability to perturb the interfacial water structure.²³ On the basis of these results and the previous SFG studies that correlated the extent of water hydrogen bonding with surface acidity,^{33,34} we were interested to determine how the bimodal distribution of silanol groups varied with the hydrated alkali ion radius. The relative amount of the acidic silanol groups is equivalent to the fraction deprotonated at pH 7, which can be determined from the relative change in $E_{2\omega}$ at low and high pH.^{29–31}

As shown in Figure 3, the fraction of more acidic silanol groups depended drastically on the identity of the alkali ion. As

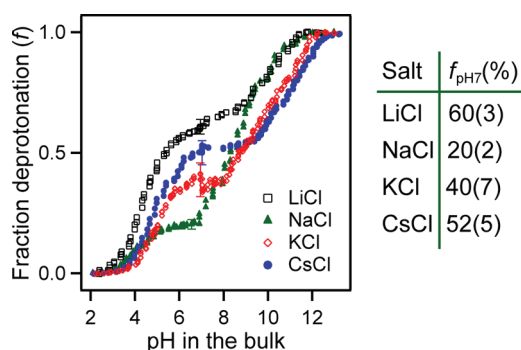


Figure 3. The fraction of deprotonated surface sites as a function of pH for the silica/electrolyte interface. Table: The percent deprotonated of the silica/electrolyte interface at pH 7.

first reported by Eisenthal and co-workers, in the presence of 0.5 M NaCl, the number of silica sites deprotonated at pH 7 represents 19% of the acidic groups, which we also observed within error for this alkali halide (Figure 3, 20(2)%). For LiCl, however, the percentage of these sites increased to 60(3)%, with KCl and CsCl exhibiting intermittent percentages of 40(7), and 52(5)%, respectively. We observed that f decreased with a decrease in the hydrated cation radius:⁴³ $f_{\text{pH}7}(\text{Li}^+) > f_{\text{pH}7}(\text{K}^+) \cong f_{\text{pH}7}(\text{Cs}^+)$, with the exception of Na^+ (Figure 3). These results support that ions with larger hydration radii must disrupt the strongly hydrogen-bonded water leading to a larger fraction of acidic sites on the surface. The deviation of sodium from the trend, however, provided further support that sodium formed unique interactions with the surface that we once again attribute to ion pair formation rather than an outer sphere complex.⁴⁴ We reason that ion-pair formation allowed water to remain strongly hydrogen bonded at the interface in the presence of these high Na^+ concentrations. Although sodium is often considered to be hydrated at colloidal silica interfaces,⁴⁵

other surface complexation models suggest that sodium can form inner sphere complexes between neighboring silanol groups such that the ion is level with the surface silanol sites, which might explain the lack of disruption of strongly hydrogen-bonded water molecules for this cation.¹²

We cannot rule out other contributions from the cations that change the bimodal distribution at the interface such as surface restructuring, which could result in a hydrophobic surface that favors more acidic silanol groups.¹⁴ Nevertheless, these results support that equilibrium behavior and the bimodal distribution of acidic sites depend strongly on the specific ion present in the aqueous phase. Thus, the binding behavior of silica should vary widely at the same pH depending on the alkali present. The trend in equilibrium constants and site distributions suggests that ion–surface, ion–water, and water–surface interactions can all play significant roles. Consequently, we expect such effects to be general for a variety of other interfaces beyond silica. As surface pK_a values are common parameters in environmental and biological models, properly modeling the influence of the electrolyte identity on interfacial acid–base equilibria will be necessary to improve model accuracy.

EXPERIMENTAL SECTION

A regeneratively amplified Ti:Sapphire laser assembly (Spectra Physics, Spitfire Pro) was used to pump an optical parametric amplifier (Spectra Physics OPA-800CF) to produce light at 550 ± 2 nm (<120 fsec, 1 kHz). After attenuation (0.3–0.5 μJ), s-polarized light was generated and focused on the interface of a fused silica hemisphere mounted on a custom-built Teflon cell, with the incident beam at 62° from surface normal. SHG ($\lambda = 275$ nm) emanating from the interface was recollimated, filtered to remove residual fundamental light, and focused onto a monochromator connected to a photomultiplier tube (PMT). The PMT electric response was then amplified and counted with a gated photon counter (Stanford Research Systems). Prior to use, the hemisphere was cleaned with sonication in water followed by methanol then water again. Next the flat surface of the hemisphere was covered with a few drops of commercially available glass cleaner Nochromix (Godax Laboratories Inc., ~ 0.25 g in 5 mL H_2SO_4) for 1 h followed by copious rinsing in Milli-Q water. The lens was then sonicated three times while immersed in Milli-Q water (5 min $\times 3$) followed by methanol (5 min), and dried in an oven at 100°C for 10 min. Finally, the cooled hemisphere was subjected to plasma cleaning (Plasma cleaner, PDC-32G, Harrick Plasma) in air for 3 min. Each silica sample was aligned in the presence of Milli-Q water before the water was replaced with the electrolyte solution. The long-term exposure of quartz to neutral water rather than pH 10 water exhibited differences in the water structure at the interface according to SFG studies that were all conducted at pH 10,⁴⁶ and so it is possible that contact with water is important to maintain the observed surface properties prior to the addition of the salt solution. Separate experiments were performed on different fresh samples for the lower and higher pH regions to avoid hysteresis.⁴⁷ We did observe that changing the starting point of the titration to different pH values led to small differences in the $\text{pH}_{0.5}$, particularly at low pH (data not shown), which suggests that hysteresis also occurs in our system. After adding the electrolyte solution, SHG was monitored for 30 min to confirm that the interface had reached equilibrium, at which point aliquots of an HCl or NaOH solution with the same electrolyte concentration were added. The resulting bulk pH was measured while allowing the sample

to equilibrate for 3 min. SHG was collected for ~2 min thereafter, and the sequence of steps was repeated.

■ ASSOCIATED CONTENT

■ Supporting Information

Additional experimental details. This material is available free of charge via the Internet at <http://pubs.acs.org>.

■ AUTHOR INFORMATION

Notes

The authors declare no competing financial interest.

■ ACKNOWLEDGMENTS

We gratefully acknowledge the Canada Foundation for Innovation and the Natural Science and Engineering Research Council for funding. We would also like to thank Paul Crothers and Dieter Stark in the Chemistry Machine Shop at the University of Alberta for machining our Teflon cell and components of our laser assembly. Finally, we thank Professor John P. Davis (U of Alberta, Physics), Professor Gabriel Hanna (U of Alberta, Chemistry) and Dr. Patrick L. Hayes (U of Colorado, Chemistry) for helpful discussions.

■ REFERENCES

- (1) Dove, P.; Craven, C. Surface Charge Density on Silica in Alkali and Alkaline Earth Chloride Electrolyte Solutions. *Geochim. Cosmochim. Acta* **2005**, *69*, 4963–4970.
- (2) Karlsson, M.; Craven, C.; Dove, P. M.; Casey, W. H. Surface Charge Concentrations on Silica in Different 1.0 m Metal-Chloride Background Electrolytes and Implications for Dissolution Rates. *Aquat. Geochem.* **2001**, *7*, 13–32.
- (3) Borah, J. M.; Mahiuddin, S.; Sarma, N.; Parsons, D. F.; Ninham, B. W. Specific Ion Effects on Adsorption at the Solid/Electrolyte Interface: A Probe into the Concentration Limit. *Langmuir* **2011**, *27*, 8710–8717.
- (4) Appelo, C. A. J.; Postma, D. *Geochemistry, Groundwater and Pollution*, 2 ed.; A. A. Balkema Publishers: Amsterdam, 2005.
- (5) Lützenkirchen, J. Comparison of 1-pK and 2-pK Versions of Surface Complexation Theory by the Goodness of Fit in Describing Surface Charge Data of (Hydr)oxides. *Environ. Sci. Technol.* **1998**, *32*, 3149–3154.
- (6) Lützenkirchen, J. The Constant Capacitance Model and Variable Ionic Strength: An Evaluation of Possible Applications and Applicability. *J. Colloid Interface Sci.* **1999**, *217*, 8–18.
- (7) Simon, S. d.; Richmond, G. L. In Situ Non-Linear Spectroscopic Approaches to Understanding Adsorption at Mineral/Water Interfaces. *J. Phys. D: Appl. Phys.* **2008**, *41*, 033001.
- (8) Campen, R. K.; Pymer, A. K.; Nihonyanagi, S.; Borguet, E. Linking Surface Potential and Deprotonation in Nanoporous Silica: Second Harmonic Generation and Acid/Base Titration. *J. Phys. Chem. C* **2010**, *114*, 8465–8473.
- (9) Corma, A.; Garcia, H. Silica-Bound Homogeneous Catalysts as Recoverable and Reusable Catalysts in Organic Synthesis. *Adv. Synth. Catal.* **2006**, *348*, 1391–1412.
- (10) Schena, M.; Shalon, D.; Davis, R. W.; Brown, P. O. Quantitative Monitoring of Gene Expression Patterns with a Complementary DNA Microarray. *Science* **1995**, *270*, 467–470.
- (11) Heise, C.; Bier, F. F. Immobilization of DNA on Microarrays. *Top. Curr. Chem.* **2006**, *261*, 1–25.
- (12) Iler, R. K. *Chemistry of Silica - Solubility, Polymerization, Colloid and Surface Properties and Biochemistry*; John Wiley & Sons: New York, 1979.
- (13) Eiseenthal, K. B. Liquid Interfaces Probed by Second-Harmonic and Sum-Frequency Spectroscopy. *Chem. Rev.* **1996**, *96*, 1343–1360.

- (14) Leung, K.; Nielsen, I. M. B.; Criscenti, L. J. Elucidating the Bimodal Acid–Base Behavior of the Water–Silica Interface from First Principles. *J. Am. Chem. Soc.* **2009**, *131*, 18358–18365.
- (15) de Beer, A.; Campen, R.; Roke, S. Separating Surface Structure and Surface Charge with Second-Harmonic and Sum-Frequency Scattering. *Phys. Rev. B* **2010**, *82*.
- (16) Zhang, Y.; Cremer, P. Interactions between Macromolecules and Ions: The Hofmeister Series. *Curr. Opin. Chem. Biol.* **2006**, *10*, 658–663.
- (17) Jungwirth, P.; Tobias, D. J. Specific Ion Effects at the Air/Water Interface. *Chem. Rev.* **2006**, *106*, 1259–1281.
- (18) Bian, H.-T.; Feng, R.-R.; Guo, Y.; Wang, H.-F. Specific Na⁺ and K⁺ Cation Effects on the Interfacial Water Molecules at the Air/Aqueous Salt Solution Interfaces Probed with Nonresonant Second Harmonic Generation. *J. Chem. Phys.* **2009**, *130*, 134709.
- (19) Kunz, W. *Specific Ion Effects*; World Scientific: Singapore, 2010.
- (20) Salis, A.; Parsons, D. F.; Bostrom, M.; Medda, L.; Barse, B.; Ninham, B. W.; Monduzzi, M. Ion Specific Surface Charge Density of SBA-15 Mesoporous Silica. *Langmuir* **2010**, *26*, 2484–2490.
- (21) Beildeck, C. L.; Steel, W. H.; Walker, R. A. Surface Charge Effects on Solvation Across Liquid/Liquid and Model Liquid/Liquid Interfaces. *Faraday Discuss.* **2005**, *129*.
- (22) Gopalakrishnan, S.; Liu, D.; Allen, H. C.; Kuo, M.; Shultz, M. J. Vibrational Spectroscopic Studies of Aqueous Interfaces: Salts, Acids, Bases, and Nanodrops. *Chem. Rev.* **2006**, *106*, 1155–1175.
- (23) Yang, Z.; Li, Q.; Chou, K. C. Structures of Water Molecules at the Interfaces of Aqueous Salt Solutions and Silica: Cation Effects. *J. Phys. Chem. C* **2009**, *113*, 8201–8205.
- (24) Kosmulski, M. The pH-Dependent Surface Charging and the Points of Zero Charge. *J. Colloid Interface Sci.* **2002**, *253*, 77–87.
- (25) Franks, G. V. Zeta Potentials and Yield Stresses of Silica Suspensions in Concentrated Monovalent Electrolytes: Isoelectric Point Shift and Additional Attraction. *J. Colloid Interface Sci.* **2002**, *249*, 44–51.
- (26) Dong, Y.; Pappu, S. V.; Xu, Z. Detection of Local Density Distribution of Isolated Silanol Groups on Planar Silica Surfaces Using Nonlinear Optical Molecular Probes. *Anal. Chem.* **1998**, *70*, 4730–4735.
- (27) O'Reilly, J. P.; Butts, C. P.; l'Anson, I. A.; Shaw, A. M. Interfacial pH at an Isolated Silica–Water Surface. *J. Am. Chem. Soc.* **2005**, *127*, 1632–1633.
- (28) Fisk, J. D.; Batten, R.; Jones, G.; O'Reilly, J. P.; Shaw, A. M. pH Dependence of the Crystal Violet Adsorption Isotherm at the Silica/Water Interface. *J. Phys. Chem. B* **2005**, *109*, 14475–14480.
- (29) Ong, S.; Zhao, X.; Eiseenthal, K. B. Polarization of Water Molecules at a Charged Interface: Second Harmonic Studies of the Silica/Water Interface. *Chem. Phys. Lett.* **1992**, *191*, 327–335.
- (30) Zhao, X.; Ong, S.; Wang, H.; Eiseenthal, K. B. New Method for Determination of Surface pKa Using Second Harmonic Generation. *Chem. Phys. Lett.* **1993**, *214*, 203–207.
- (31) Konek, C. T.; Musorrafati, M. J.; Al-Abadleh, H. A.; Bertin, P. A.; Nguyen, S. T.; Geiger, F. M. Interfacial Activities, Charge Densities, Potentials, and Energies of Carboxylic Acid-Functionalized Silica/Water Interfaces Determined by Second Harmonic Generation. *J. Am. Chem. Soc.* **2004**, *126*, 11754–11755.
- (32) Du, Q.; Freysz, E.; Shen, Y. Vibrational Spectra of Water Molecules at Quartz/Water Interfaces. *Phys. Rev. Lett.* **1994**, *72*, 238–241.
- (33) Ostroverkhov, V.; Waychunas, G.; Shen, Y. New Information on Water Interfacial Structure Revealed by Phase-Sensitive Surface Spectroscopy. *Phys. Rev. Lett.* **2005**, *94*.
- (34) Du, Q.; Freysz, E.; Shen, Y. R. Vibrational Spectra of Water Molecules at Quartz/Water Interfaces. *Phys. Rev. Lett.* **1994**, *72*, 238–241.
- (35) Duval, Y.; Mielczarski, J. A.; Pokrovsky, O. S.; Mielczarski, E.; Ehrhardt, J. J. Evidence of the Existence of Three Types of Species at the Quartz/Aqueous Solution Interface at pH 0–10: XPS Surface Group Quantification and Surface Complexation Modeling. *J. Phys. Chem. B* **2002**, *106*, 2937–2945.

- (36) Pearson, R. G. Hard and Soft Acids and Bases, HSAB, Part 1: Fundamental Principles. *J. Chem. Educ.* **1968**, *45*, 581.
- (37) Collins, K. D. Ion Hydration: Implications for Cellular Function, Polyelectrolytes, and Protein Crystallization. *Biophys. Chem.* **2006**, *119*, 271–281.
- (38) CRC *Handbook of Chemistry and Physics*, 92 ed.; CRC Press: Boca Raton, FL, 2011.
- (39) Chen, X.; Yang, T.; Kataoka, S.; Cremer, P. S. Specific Ion Effects on Interfacial Water Structure near Macromolecules. *J. Am. Chem. Soc.* **2007**, *129*, 12272–12279.
- (40) Onorato, R. M.; Otten, D. E.; Saykally, R. J. Adsorption of Thiocyanate Ions to the Dodecanol/Water Interface Characterized by UV Second Harmonic Generation. *Proc. Natl. Acad. Sci. U.S.A.* **2009**, *106*, 15176–15180.
- (41) Collins, K. D.; Washabaugh, M. W. The Hofmeister Effect and the Behaviour of Water at Interfaces. *Q. Rev. Biophys.* **1985**, *18*, 323–422.
- (42) Cacace, M. G.; Landau, E. M.; Ramsden, J. J. The Hofmeister Series: Salt and Solvent Effects on Interfacial Phenomena. *Q. Rev. Biophys.* **1997**, *30*, 241–277.
- (43) Kielland, J. Individual Activity Coefficients of Ions in Aqueous Solutions. *J. Am. Chem. Soc.* **1937**, *59*, 1675–1678.
- (44) Rahnamaie, R.; Hiemstra, T.; van Riemsdijk, W. H. A New Surface Structural Approach to Ion Adsorption: Tracing the Location of Electrolyte Ions. *J. Colloid Interface Sci.* **2006**, *293*, 312–321.
- (45) Parsons, D. F.; Boström, M.; Maceina, T. J.; Salis, A.; Ninham, B. W. Why Direct or Reversed Hofmeister Series? Interplay of Hydration, Non-electrostatic Potentials, and Ion Size. *Langmuir* **2009**, *26*, 3323–3328.
- (46) Li, I.; Bandara, J.; Shultz, M. J. Time Evolution Studies of the H₂O/Quartz Interface Using Sum Frequency Generation, Atomic Force Microscopy, and Molecular Dynamics. *Langmuir* **2004**, *20*, 10474–10480.
- (47) Gibbs-Davis, J. M.; Kruk, J. J.; Konek, C. T.; Scheidt, K. A.; Geiger, F. M. Jammed Acid–Base Reactions at Interfaces. *J. Am. Chem. Soc.* **2008**, *130*, 15444–15447.